ELSEVIER

Polymer Vol. 37 No. 2, pp. 213–218, 1996

0032-3861/96/$15.00+0.00

On the formation of defects in drawn polypropylene fibres

M. I. Abo El Maaty*, D. C. Bassett† and R. H. Olley
J.J. Thomson Physical Laboratory, University of Reading, Reading RG6 2AF, UK

and M. G. Dobb, J. G. Tomka and I.-C. Wang‡
Department of Textile Industries, University of Leeds, Leeds LS2 9JT, UK
(Received 16 May 1995)

Drawn polypropylene fibres were produced from as-spun fibres with a paracrystalline structure of low orientation. Drawing was carried out at 60°C in order to prevent the transformation of the paracrystalline form into the monoclinic structure. The internal texture of the as-spun fibre and of a series of drawn fibres has been investigated by electron microscopy following permanganic etching. At draw ratios of 7 and above a series of transverse bands can be observed along the fibres. Homogeneous regions alternate with bands of defects which, after etching, appear as longitudinal cavities. Defect bands become more regular and increase in height with increasing draw ratio, λ, occupying almost all the sample at $\lambda = 8.3$. The nature of the defects, which are regions of reduced density, possibly voids, is discussed and a simplified model for their formation is suggested.

(Keywords: polypropylene; fibres; drawing)

INTRODUCTION

In common with other fibres produced from linear flexible-chain polymers by melt-spinning followed by drawing, the structure and properties of polypropylene fibres are strongly influenced by the fibre formation conditions[1]. In 1964, Sheehan and Cole[2] established that maximum tenacity is achieved by optimized drawing of paracrystalline as-spun fibres of low orientation. This has been subsequently confirmed by others[3].Technologically feasible conditions for producing as-spun fibres of the required structure have now been identified and systematic investigations aimed at optimizing the drawing conditions have been carried out[4,5]. It has been established that a two-stage drawing process is a feasible route for producing polypropylene continuous filament yarns of high tenacity ($\sim 0.9\,\mathrm{N\,tex^{-1}}$; $1\,\mathrm{tex} = 1\,\mathrm{g\,km^{-1}}$). The first stage is carried out at a sufficiently low temperature (e.g. 60°C) to prevent a premature transformation of the paracrystalline structure into the monoclinic form. During the second stage, carried out at a higher temperature (e.g. 140°C), the oriented paracrystalline structure is transformed into the oriented monoclinic form. Investigation of the first-stage drawing revealed a noticeable difference in the appearance of the drawn fibres at high draw ratios. The fibres became opaque and appeared to be delustred. This 'chalking' or 'whitening' phenomenon is well known in technological practice and it has been ascribed tentatively to the formation of microvoids[3]. However, so far it has not been investigated using advanced microscopic techniques.

Recent studies[6–9] of a variety of polymeric fibres have revealed the widespread presence of internal longitudinal defects, usually several micrometres in length. These are not voids but regions of reduced density, whose excess free volume renders them prone to earlier melting than their surroundings[9]. They were first identified within compacted high-modulus polyethylene fibres produced by melt-spinning followed by drawing[7]. Subsequent studies have shown that similar phenomena occur within several, but not all, polymeric systems as well as in individual fibres, even before compaction[10]. These include various high-performance polyethylene fibres, prepared by different routes, and poly(ethylene terephthalate)[11] but so far not aramid or aromatic copolyesters (unpublished work in progress). In such systems, where defects are present in the initial fibres, their origin has been related to the circumstances of crystallization. When polypropylene fibres were examined[10,12] somewhat similar defects were found in etched transverse sections but only in fibres with higher draw ratios and not the as-spun precursor. In fact, these longitudinal defects form and develop during tensile drawing of initially defect-free polypropylene fibres. In this paper we report on a preliminary investigation of this topic.

EXPERIMENTAL

The as-spun fibres were produced from FINA 10080S

* Present address: Department of Physical Science, Faculty of Engineering, University of Mansoura, Mansoura, Egypt
† To whom correspondence should be addressed
‡ Present address: Chung Shing Textile Co Ltd, Taiwan, Republic of China

Table 1 Polypropylene fibres: applied draw ratio, λ; actual draw ratio, λ_a; optical birefringence, Δn

Sample	λ	λ_a	Δn
1	[a]	1.00	0.0025
2	3.0		
3	4.1	4.02	0.0283
4	7.0	6.74	0.0310
5	8.3	7.86	

[a] As-spun fibre (undrawn)

granules of melt flow index 35 g/10 min (ASTM D1238; 2.16 kg/230°C) using a Fourne Spintester with a spinneret containing 12 holes (diameter 510 μm, length 1020 μm). The extrusion temperature was 280°C and the winding speed was 200 m min^{-1}. The throughput was adjusted to produce yarns of linear density of around 25 tex. The as-spun fibres were drawn using a Dienes Drawframe equipped with a heated feed roll (60°C); the draw roll speed was set at 210 m min^{-1}. The applied draw ratios, λ, were between 3.0 and 8.3 (see *Table 1*). The actual draw ratios, λ_a, were calculated from the decrease of linear density resulting from drawing. The nature of the crystalline structure of both as-spun and drawn fibres was determined from wide-angle X-ray diffraction patterns. The optical birefringence was evaluated using a Pluta polarizing interference microscope[13].

All samples were examined by electron microscopy. To this end, fibres were embedded in Kraton 1650 block copolymer (Shell Petroleum) to form composite specimens. Blocks of these were then cut both transversely and longitudinally to the fibre axis using a glass-knife in a microtome. Specimens with cut surfaces were etched with a permanganic reagent (0.7% $KMnO_4$ in 10:4:1 H_2SO_4:H_3PO_4:H_2O) for 2 h at room temperature then washed according to standard procedures[14]. The etched cut surfaces were either examined directly by scanning electron microscopy (SEM) or indirectly via two-stage replication using transmission electron microscopy (TEM) for higher resolution. Unless stated otherwise, all illustrations are of the interior of fibres, after etching.

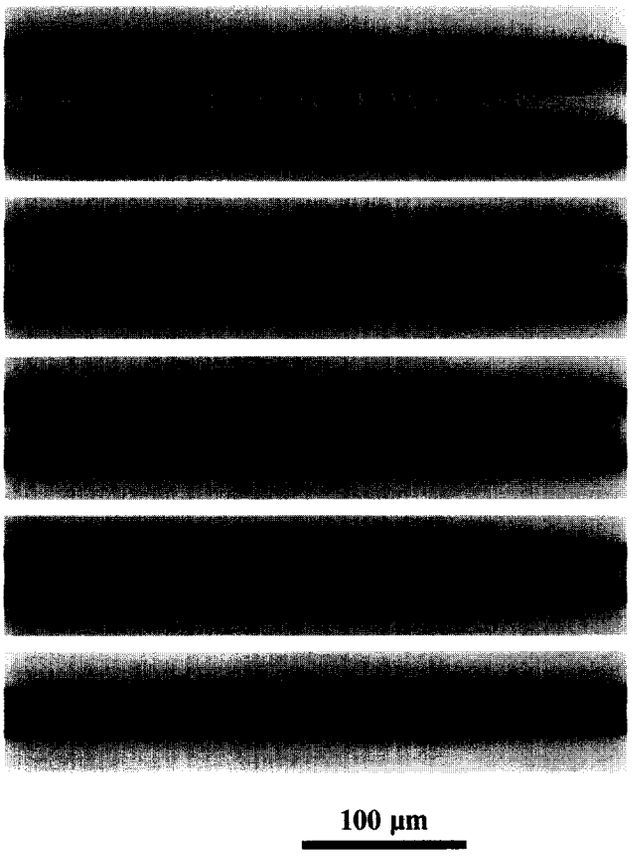

Figure 1 Optical bright field micrographs of the five fibres examined, from sample 1 at the top to sample 5 at the bottom

RESULTS

Wide-angle X-ray scattering patterns showed that the as-spun fibre is paracrystalline and almost isotropic. Subsequent drawing caused an increase in orientation, but the structure remained paracrystalline. At a draw

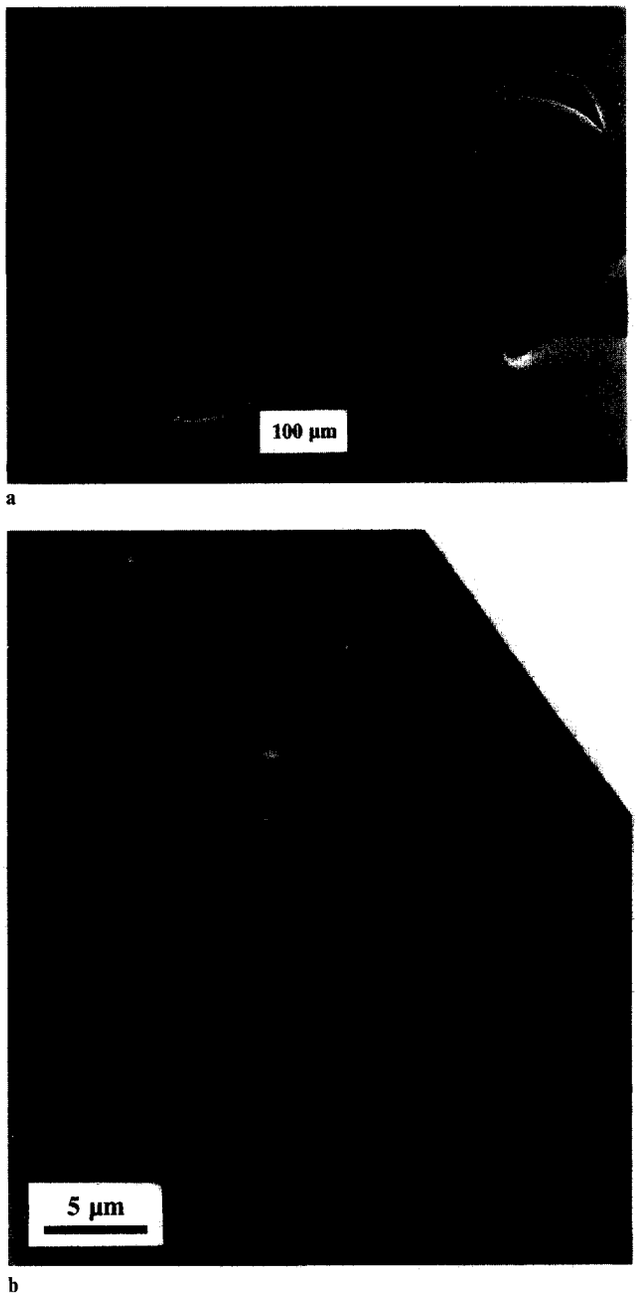

Figure 2 (a) Etched transverse section of the precursor fibre (sample 1) embedded in a rubber matrix, showing the absence of defects. Scanning electron micrograph. (b) Etched longitudinal section of (a); replica

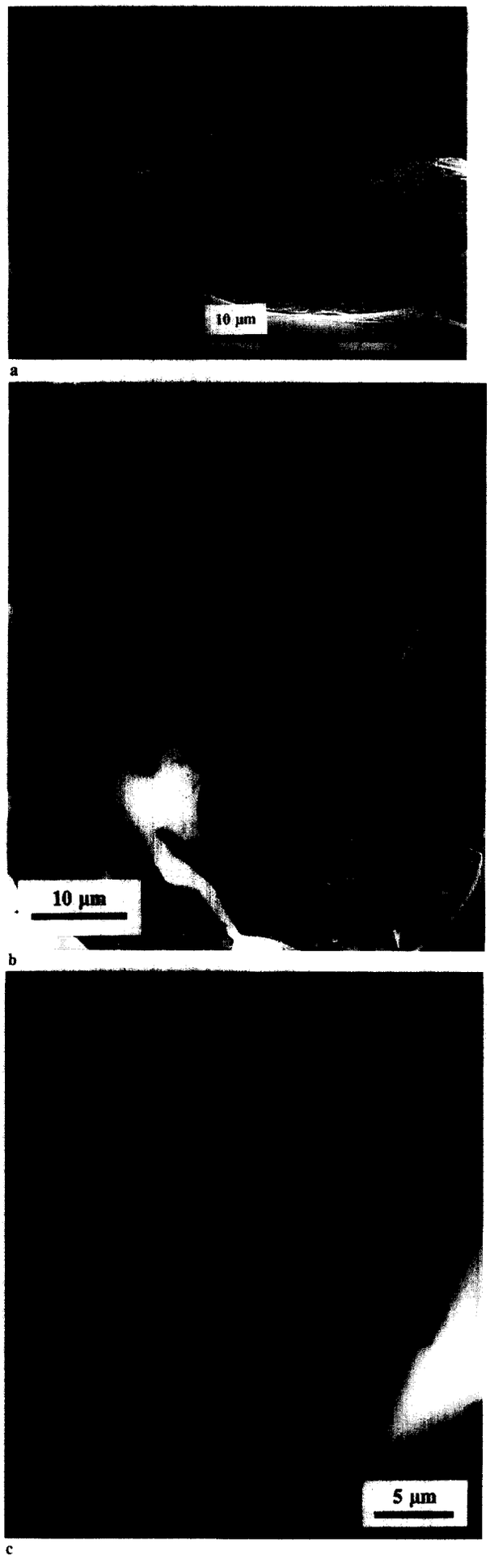

ratio $\lambda = 8.3$ the fibres displayed the whitening previously mentioned. The changing optical appearance of all the fibres examined is shown in *Figure 1*.

Electron microscopy of the as-spun fibres (sample 1) indicates that they are essentially featureless and homogeneous both in transverse (*Figure 2a*) and longitudinal (*Figure 2b*) section. However, even at low draw ratios, some internal texture is present. In etched cross-sections both samples 2 ($\lambda = 3$; *Figure 3a*) and 3 ($\lambda = 4.1$; *Figure 3b*) are cratered, sometimes deeply so, and appear similar to the defect regions in polyethylene fibres[7]. Longitudinal sections contain etched pits of characteristic shape (*Figure 3c*). They resemble two blunt-ended cones joined base to base, with some tendency to bulge at the common junction. A comparison of the number and distribution of defects suggests that it may be only the deepest craters in *Figure 3b* which correspond to the etched pits in *Figure*

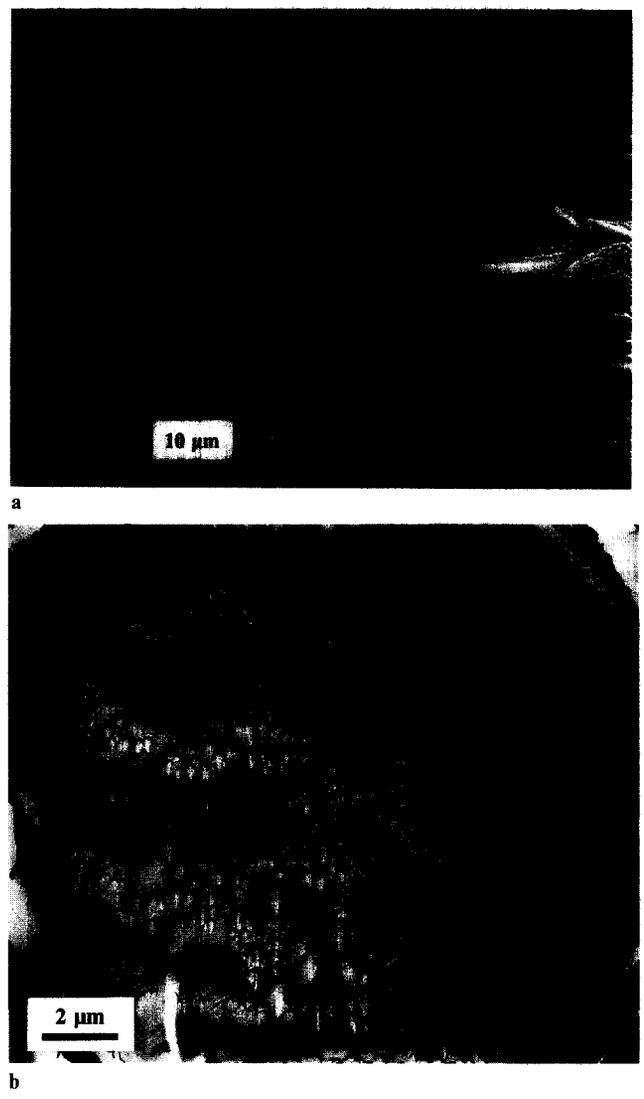

Figure 4 (a) Oblique view of etched cross-sections of fibre 4 showing the variability of deformed texture. Scanning electron micrograph. (b) Detail of one etched cross-section of fibre 4; replica

Figure 3 (a) A few defects are visible in etched cross-sections of fibre 2. Scanning electron micrograph. (b) Defect structures in etched cross-sections of fibre 3 seen with the higher resolution of TEM; replica. (c) Longitudinal section of fibre 3; replica

3c. (These are identifiable by the presence of dark, residual replicating material which casts a prominent shadow.)

In contrast to the small number and scattered distribution of defects in samples 2 and 3, those in samples 4 and 5 are many and are spatially ordered. *Figure 4a*, which is an oblique view of a group of etched cross-sections of fibre 4, reveals much cratering although there is a considerable variation in the textures exposed. Finer details of pitting in one etched fibre (seen in reversed contrast) are shown in *Figure 4b*. These views make the point that the defects, which etching develops into craters, have become much more numerous at a draw ratio of 7.

Longitudinal sections (*Figure 5a*) show that the defects are arranged in bands normal to the fibre axis. To a first approximation, bands of etched troughs alternate with regions of low contrast which appear homogeneous. Note that here the embedding medium is raised between fibres whereas in etched cross-sections, such as in *Figure 4*, it is generally etched more than the fibres. This suggests that these polypropylene fibres are etched at a faster rate laterally than longitudinally.

For sample 4 the height of the defect bands is comparable to that of adjacent homogeneous bands but may be more or less according to region, as shown in *Figures 5a* and *5b*. At higher magnification (*Figure 5c*) it is clear that beyond the etched bands, at approximately 0.2 μm into the 'homogeneous' region, there is a change of shadow contrast identifying a line of indentation into the etched surface of the fibre.

The fibre with largest draw ratio ($\lambda = 8.3$), sample 5, shows regular bands of defects developed to an extent where they occupy almost all the sample. Etched cross-sections (*Figure 6a*) reveal high densities of defects, with some inhomogeneity of coverage. Note that adjacent fibres have different number densities of etched pits, that these may be arranged in lines but mostly appear to be in quasi-random array, and that not all pits appear in dark contrast; in some areas they are grey. There are few, if any, etched pits within about 1 μm of the external surface, consistent with a less-defected skin region of this thickness.

The complementary longitudinal section (*Figure 6b*) shows transverse bands of etched cavities, each aligned along the fibre axis. These are separated by narrow, apparently intact regions. Some cavities may have complex geometries, resulting from the incorporation or merger of smaller units (e.g. in the largest cavity to the lower left of *Figure 6b*).

Some of the uniform transverse regions (*Figure 7a*) extend across the whole width of the fibre, almost to the edge. Others, towards the top and on the right just below centre in *Figure 7b*, appear to terminate part way through the fibre but have a hint of their presence manifested by the lack of continuity of etched cavities across their projected path. This is the final stage of conversion to a fibre with few defects into one full of longitudinal defects. Intermediate stages, as in *Figure 5*, consist essentially of defective and homogeneous transverse bands connected in series along the fibre.

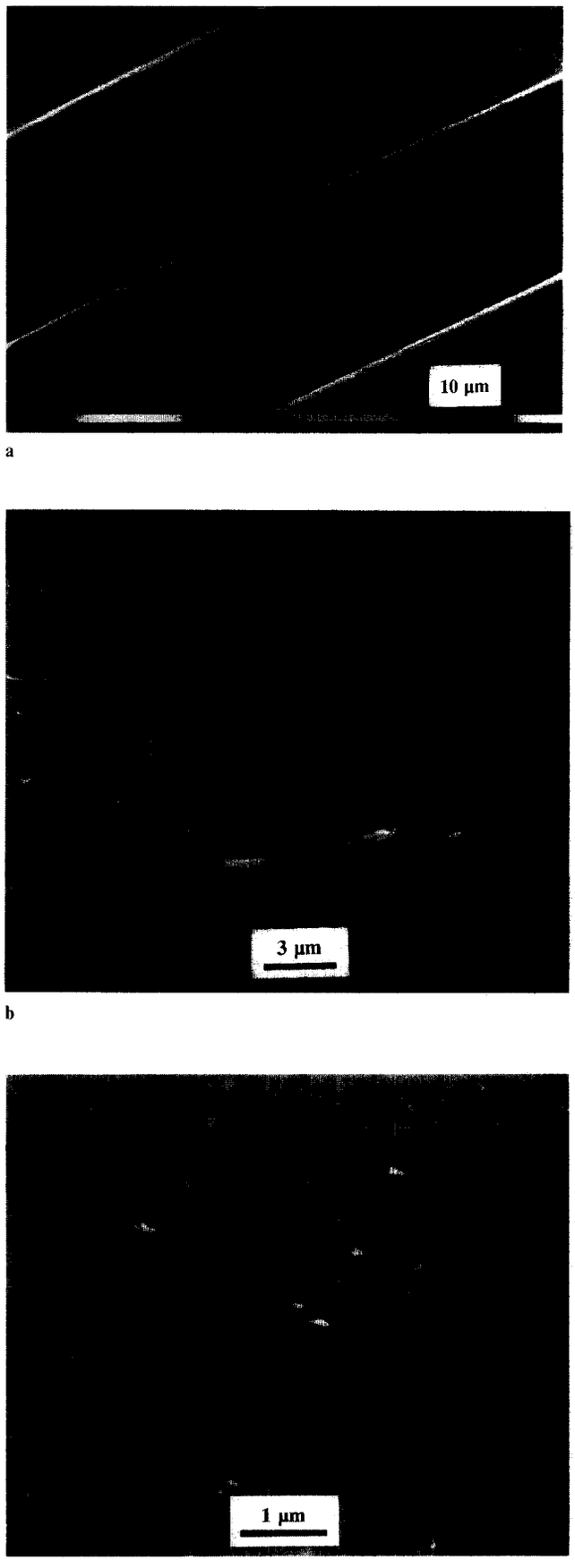

Figure 5 (a) Etched longitudinal section of fibre 4 showing the alternation of homogeneous and defective bands and their location within the fibre. Scanning electron micrograph. (b) An etched longitudinal section of fibre 4 seen at higher resolution; replica. (c) Detail of individual defects in a similar area to (b)

DISCUSSION

The existence of heterogeneities in refractive index, with

dimensions of the order of the wavelength of light ($\sim 0.5\ \mu m$) is implied by the well known phenomenon of strain-whitening present in polypropylene fibres drawn to higher extensions. So far as we are aware, however, the nature of these heterogeneities and their location have not previously been identified in the form observed here. What has been reported is the presence of transverse lines in deformed polypropylene fibres, e.g. ref. 15, and, in one instance, features apparently resembling some of those we have observed but at lower resolution[16].

In this first examination the texture within polypropylene fibres has only been observed indirectly, using permanganic etching. Although etching is likely to modify what is being observed, e.g. by deepening and broadening defective regions, the nature of the unmodified texture may still be inferred. Relief in the sample is revealed by preferential etching which implies, in the present context, greater penetrability by the permanganic etchant, i.e. lower density than the surrounding material. In previous work on polyethylene fibres an apparently similar microstructure was confirmed both by the earlier melting of reduced density regions and by the localization of the density deficit into a central hole following local melting and recrystallization[9]. Here we may be confident, from the longitudinal sections of samples 4 and 5 (*Figures 4*, *5c* and *6*), that the defects are parallel-sided. The observed lengths will be close to those before etching but their widths may well have been significantly enlarged during their treatment.

The lengths of defects appear, particularly on the evidence of *Figure 5*, to fall into two populations. The majority forms transverse bands, about 1 μm high, along the fibre axis. There is also a small number of longer (and wider) defects a few micrometres long. The two longest in *Figure 5b* both show some oscillation of width and may possibly be a development of the defects seen in samples 2 and 3, e.g. in *Figure 3c*, which are also long and not associated in bands. In discussing the formation of defects we shall confine ourselves to those which comprise transverse bands.

The presence of alternating homogeneous and defective bands transverse to the fibre is a most salient observation. A series arrangement indicates bistability such as would result from the schematic diagram of *Figure 8* and, indeed, the data of Garton *et al.* do have this form of force/extension curve[16]. In the nomenclature of *Figure 8* the fibre experiences a maximum force F_0 at a

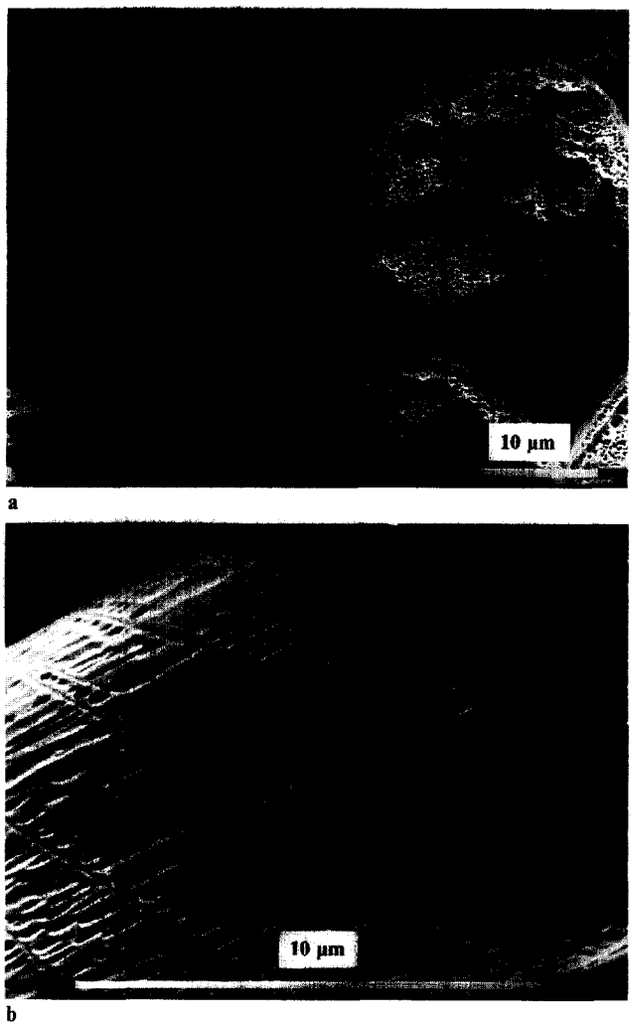

Figure 6 (a) Etched cross-sections of fibre 5. Note the variability of detail within and between fibres. Scanning electron micrograph. (b) Relief in an etched longitudinal section of fibre 5. Scanning electron micrograph

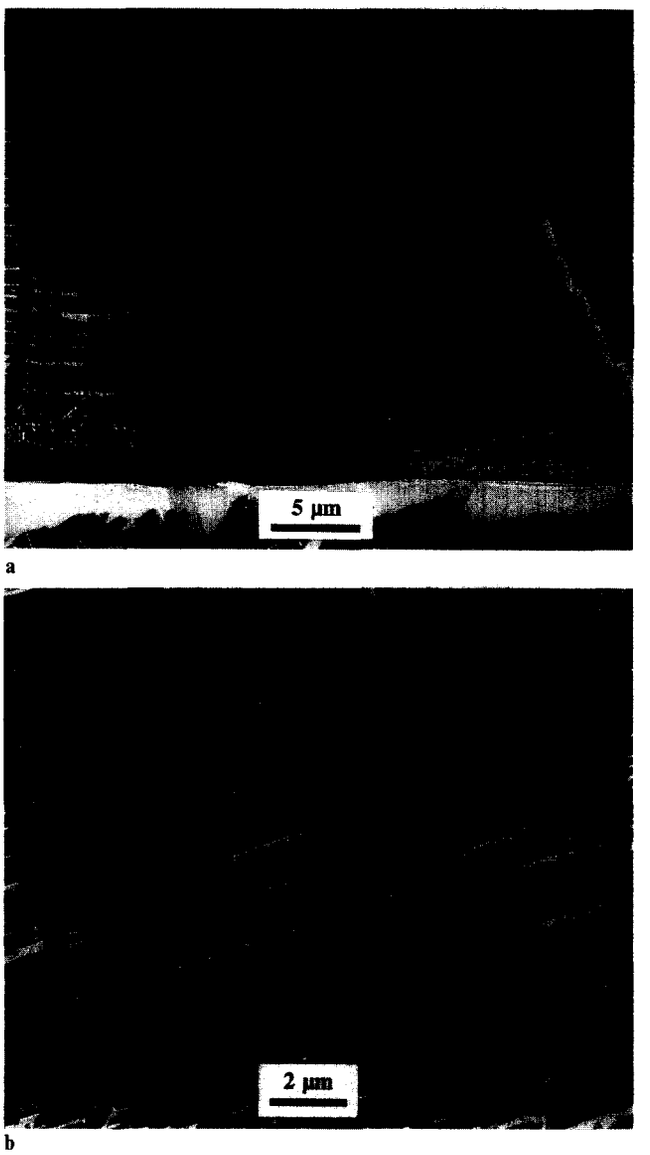

Figure 7 (a) In fibre 5 defective regions occupy almost all the sample; replica of an etched longitudinal section. (b) Detail of (a)

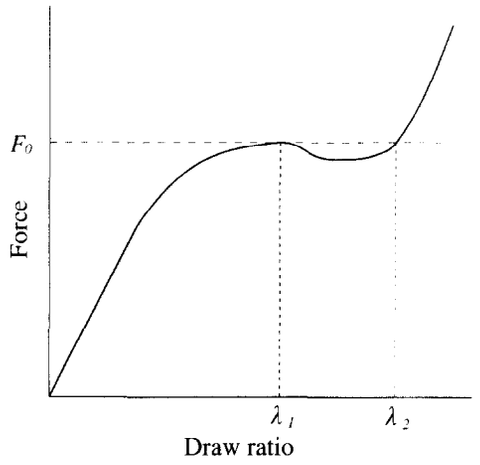

Figure 8 Schematic force/extension curve of a fibre to generate a series yielded morphology

draw ratio λ_1, a value which does not recur until the higher draw ratio λ_2. This simple model is a first approximation to the drawing behaviour of our fibres. It implies that yield will begin at λ_1 and stability will only be regained at λ_2 so that regions of draw ratio λ_1 and λ_2 will occur in series. This argument is that used in the well known Considère construction predicting the onset of necking. In that case a reduction in cross-section of approximately λ_1/λ_2 occurs at the neck in order to keep the density constant. In our fibres, by contrast, the cross-section itself is effectively constant and the requirement to maintain density in regions with $\lambda > \lambda_1$ has been met instead by internal yielding to the biaxial transverse tensile stresses tending to reduce the cross-section. The result is arrays of cylindrical yielded regions within an effectively homogeneous matrix, paralleling the way in which meshes are manufactured commercially. That there is internal yielding must imply that the fibre has reached a condition of transverse weakness, presumably because of reduced covalent connections. The anticipated failure modes would produce longitudinal defects, either empty voids, as is commonly supposed, or craze-like features with transverse connections across them, when strain-hardening could limit the width of defects. It is not yet possible, with information only for etched specimens, to be more precise about the actual microstructure of the defects. That will come with direct TEM examination of thin sections of drawn fibres.

Pursuing this model, we infer that fibres 4 and 5 have been drawn beyond λ_1 and consist of alternating homogeneous and defective regions of draw ratio λ_1 and λ_2 respectively. If the proportion of homogeneous bands in fibre 4 is taken to be 0.5 on average and, similarly, 0.1 in fibre 5, then solution of the two simultaneous equations for λ readily yields $\lambda_1 = 5.4$ and $\lambda_2 = 8.6$. For $\lambda_1 < \lambda < \lambda_2$ the defects would grow longitudinally to occupy the appropriate proportion of the fibre length. Their number would be at least that appropriate to voids in a matrix of constant density material, i.e. giving a fraction $(1 - \lambda_1/\lambda_2)$ of the cross-sectional area, roughly one-third in this instance. An estimation of the proportion of defects from *Figure 6a* would not give a higher figure than one-third, implying that the defects are probably close to being voids. At this stage there is no information as to whether or not there is also lateral bridging.

The model as so far presented is consistent with observation except in one important respect. This concerns the fibre diameter, which for a simple series model would remain constant, at that for λ_1, for all higher draw ratios. This is contrary to observation which shows that the fibre diameter continued to decrease uniformly beyond λ_1 (*Figure 1*).

The implication of the reducing cross-section at constant or increased force is that the bands in the fibre, both homogeneous and defective, are sustaining a higher stress, i.e. strain-hardening has occurred. Accordingly, λ_1, the draw ratio to yield, is not constant but is an increasing function of draw ratio, as must also be λ_2, the higher draw ratio with which a homogeneous deformation of λ_1 is in mechanical equlibrium. One needs, therefore, to recognize that yielding can occur over a range of draw ratios according to longitudinal variations in strength. According to the Considère construction, this condition would occur when the applied force is independent of draw ratio.

CONCLUSIONS

This paper has shown that:

1. longitudinal defects develop within polypropylene fibres during drawing;
2. at draw ratios of 7 and above, fibres contain transverse bands of defects alternating with homogeneous areas along the length of the fibre;
3. defect bands increase in length and proportion with draw ratio, until they occupy practically all the sample;
4. the defects are regions of reduced density, probably voids, for the formation of which a simple model is suggested.

REFERENCES

1 Ziabicki, A. 'Fundamentals of Fibre Formation', Wiley, London, 1976
2 Sheehan, W. C. and Cole, T. B. *J. Appl. Polym. Sci.* 1964, **8**, 2359
3 Ahmed, M. 'Polypropylene Fibres Science and Technology', Elsevier, Amsterdam, 1982
4 Murata, M. MSc Thesis, The University of Leeds, 1991
5 Wang, I.-C. PhD Thesis, The University of Leeds, 1994
6 Hine, P. J., Ward, I. M., Olley, R. H. and Bassett, D. C. *J. Mater. Sci.* 1993, **28**, 316
7 Olley, R. H., Bassett, D. C., Hine, P. J. and Ward, I. M. *J. Mater. Sci.* 1993, **28**, 1107
8 Kabeel, M. A., Bassett, D. C., Olley, R. H., Hine, P. J. and Ward, I. M. *J. Mater. Sci.* 1994, **29**, 4694
9 Kabeel, M. A., Bassett, D. C., Olley, R. H., Hine, P. J. and Ward, I. M. *J. Mater Sci.* 1995 **30**, 601
10 Abo El Maaty, M. I. PhD Thesis, University of Mansoura, 1995
11 Rasburn, J., Hine, O. J., Ward, I. M., Olley, R. H., Bassett, D. C. and Kabeel, M. A. *J. Mater. Sci.* 1995, **30**, 615
12 Abo el Maaty, M. I., Bassett, D. C., Olley, R. H., Hine, P. J. and Ward, I. M. *J. Mater. Sci.* in press
13 Hamza, A. A. *Textile Res. J.* 1983, **53**, 205
14 Olley, R. H., Hodge, A. M. and Bassett, D. C. *J. Polym. Sci. Phys. Edn.* 1979, **17**, 627
15 Samuels, R. J. *J. Polym. Sci. A-2* 1965, **6**, 2021
16 Garton, A., Carlsson, D. J., Sturgeon, P. Z. and Wiles, D. M. *J. Polym. Sci., Polym. Phys. Edn.* 1977, **15**, 2013